Supplemental Figures

Fig. S1 Selection of Motifs from ChIP-seq Datasets to Test KIKO Binding to HRE

ChIP-seq datasets in the vicinity of uterine focus genes in Figs. 2 and 5-7 are displayed in UCSC Genome Browser showing WT and KIKO ERα (Blue), and PR (red) ChIP-seq tracks from mice treated for one hour with vehicle, E_2 or P_4, and input tracks (blue). The arrow shows the HRE or ERE motif containing peak and the motif sequence that was inserted in pGL4.23 plasmid and tested in the *in vitro* DNA binding assay is shown. HRE or ERE motifs are indicated by bold text with consensus-matching nucleotides underlined.

A) Ihh

B) Igf1

C) Aqp5 +2400 negative control

ChIP-seq near *Aqp5* showing selection of negative ChIP-PCR primers (region in oval)

ChIP-PCR using negative control primers

Fig. S2 Control vectors demonstrate specificity of reporter gene assays

WT, KIKO and EAAE ERα with empty pGL4.23-luc vector, EBNA-luc, *Igf1* NRE-luc, *Fkbp5* NRE-luc. Fold changes relative to V are indicated above each bar. E_2 10 nM, P_4 100 nM. Note that PR induction of empty pGL4.23 or EBNA-luc is similar to PR induction of *Igf1* ERE-luc (Fig. 5*B*), indicating the activity may be mediated by a cryptic PR site in the vector. Statistics: 2-way ANOVA, multiple comparisons of means vs. V, Bonferroni multiple test correction, *p<0.05, ** p<0.001***p<0.001, **** p<0.0001

Fig. S3 Epstein Barr Virus Nuclear Antigen (EBNA) motif does not disrupt KIKO ERα HRE or ERE complex

Since the NRE motif disrupted KIKO ERα complexes with HRE or ERE, to demonstrate the specificity of the DNA binding assay, 10x excess un-biotinylated EBNA motif was included in the binding reaction. Biotinylated *Fkbp5* HRE, *Ihh* HRE or *Igf1* ERE binding with nuclear protein extracts from WT or KIKO uteri. ERα-DNA complexes were detected as described in materials and methods. Non-biotinylated (unlabeled) DNA (Positive controls*: Fkbp5* HRE, *Ihh* HRE or *Igf1* ERE, Negative controls*: Fkbp5* NRE or *Igf1* NRE or EBNA; sequences in Table S1) was added to binding reactions at 10x higher levels to compete with biotinylated probes for ERα binding and demonstrate specificity. Probe, no NE sample contained no nuclear extract. Statistics: 2-way ANOVA, multiple comparisons of values to binding reactions without unlabeled competitor DNA (none), Bonferroni multiple test correction,* P<0.05, ** P<0.01,***P<0.001 **** p<0.0001.

Fig. S4 EAAE ERα Mouse Uterus Lacks Transcriptional Responses to E_2

A. RT-PCR analysis of transcripts in WT and EAAE uterine samples treated for 2h with saline or E_2. Transcripts that were E_2 responsive in the KIKO uterus (1) were selected for analysis in the EAAE uterus. Statistics: 2-way ANOVA, multiple comparisons of means vs. V, Bonferroni multiple test correction, *p<0.05, ** p<0.001***P<0.001, **** p<0.0001.

B. Western blot of WT and EAAE uterine proteins probed with anti ERα and normalized to β-tubulin. ERα/βTub represents the ratio of the respective signal intensities.

C. EAAE differentially expressed uterine transcripts. Cluster showing 53 probes (representing 44 genes) that were differentially expressed (FDR<0.05, fold change >2.0) in EAAE.

D. Hierarchical cluster comparing previous microarray data from KIKO (1) to EAAE.

As the older KIKO dataset and 2 WT datasets were done using a 2-color protocol (1), whereas the newer EAAE and 1 WT datasets were done using a one-color protocol (Materials and methods), to make this comparison, values are expressed as log10(ratio E_2 2h/veh) and normalized to mean=0, SD=1.0. Cluster represents 7093 probes with at least 2-fold change (ratio >2.0 or <0.5), and filtered to remove probes with ratio=0 in the older dataset.

References

1. Hewitt SC, O'Brien JE, Jameson JL, Kissling GE, Korach KS. Selective Disruption of ER alpha DNA-Binding Activity Alters Uterine Responsiveness to Estradiol. *Molecular Endocrinology.* 2009;23(12):2111-2116.

Fig. S1A. *Ihh*

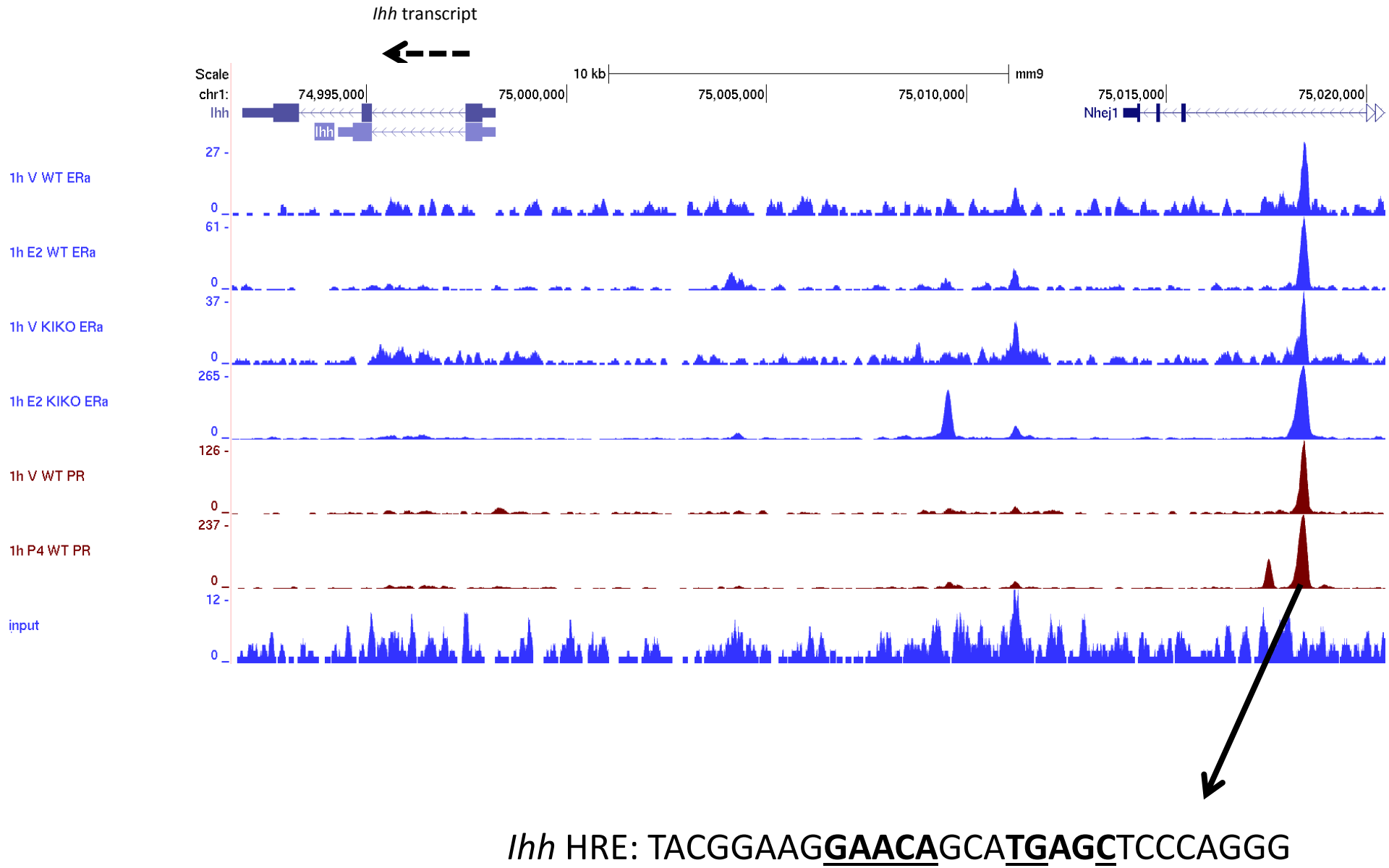

Ihh HRE: TACGGAAG**GAACA**GCA**TGAGC**TCCCAGGG

Fig. S1*B*. *Igf1*

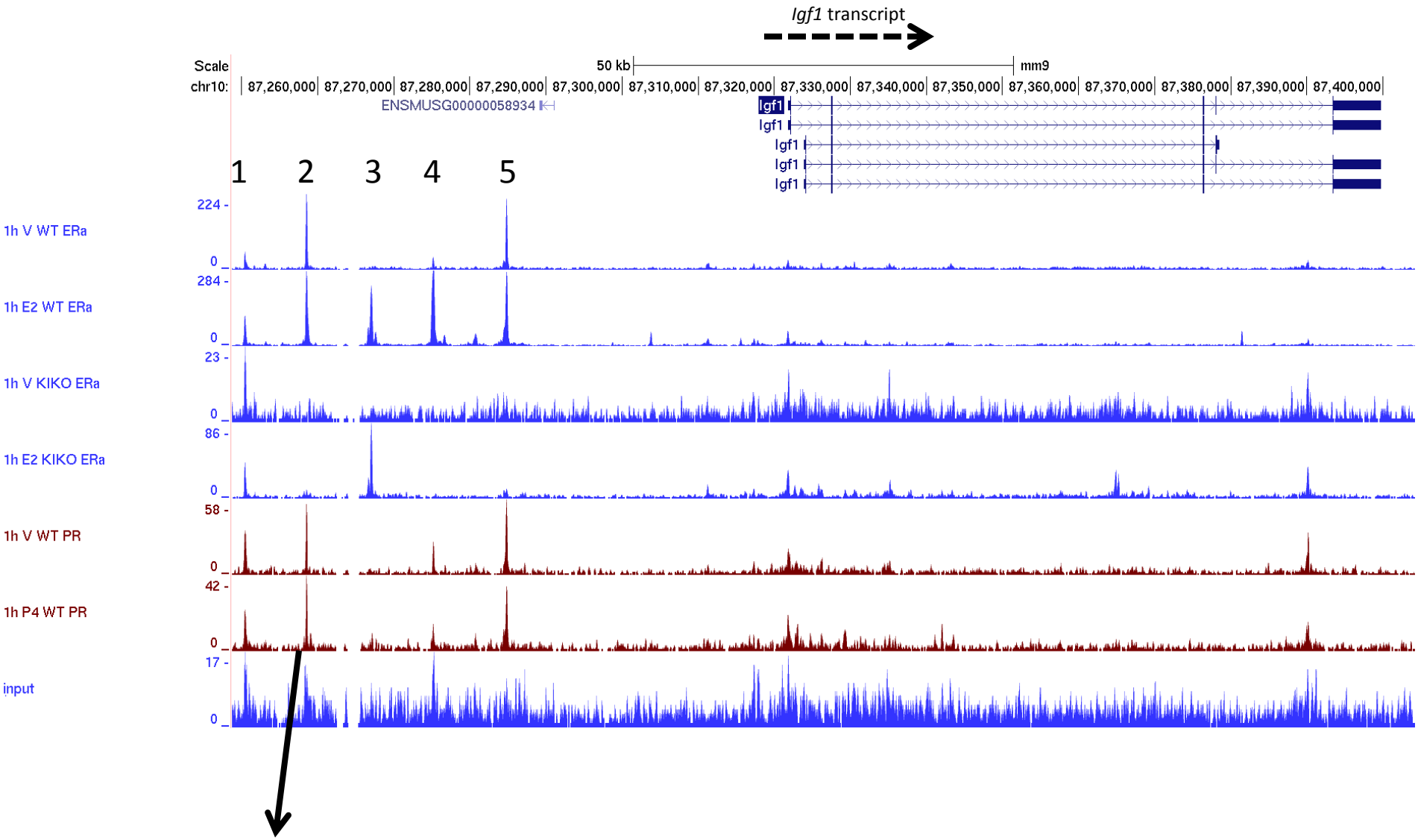

Igf1 ERE:
CTGGGCAA**GGTCA**TGA**TGACC**GCTGTATTT

Fig. S1C *Aqp5 +2400 (negative primers)*

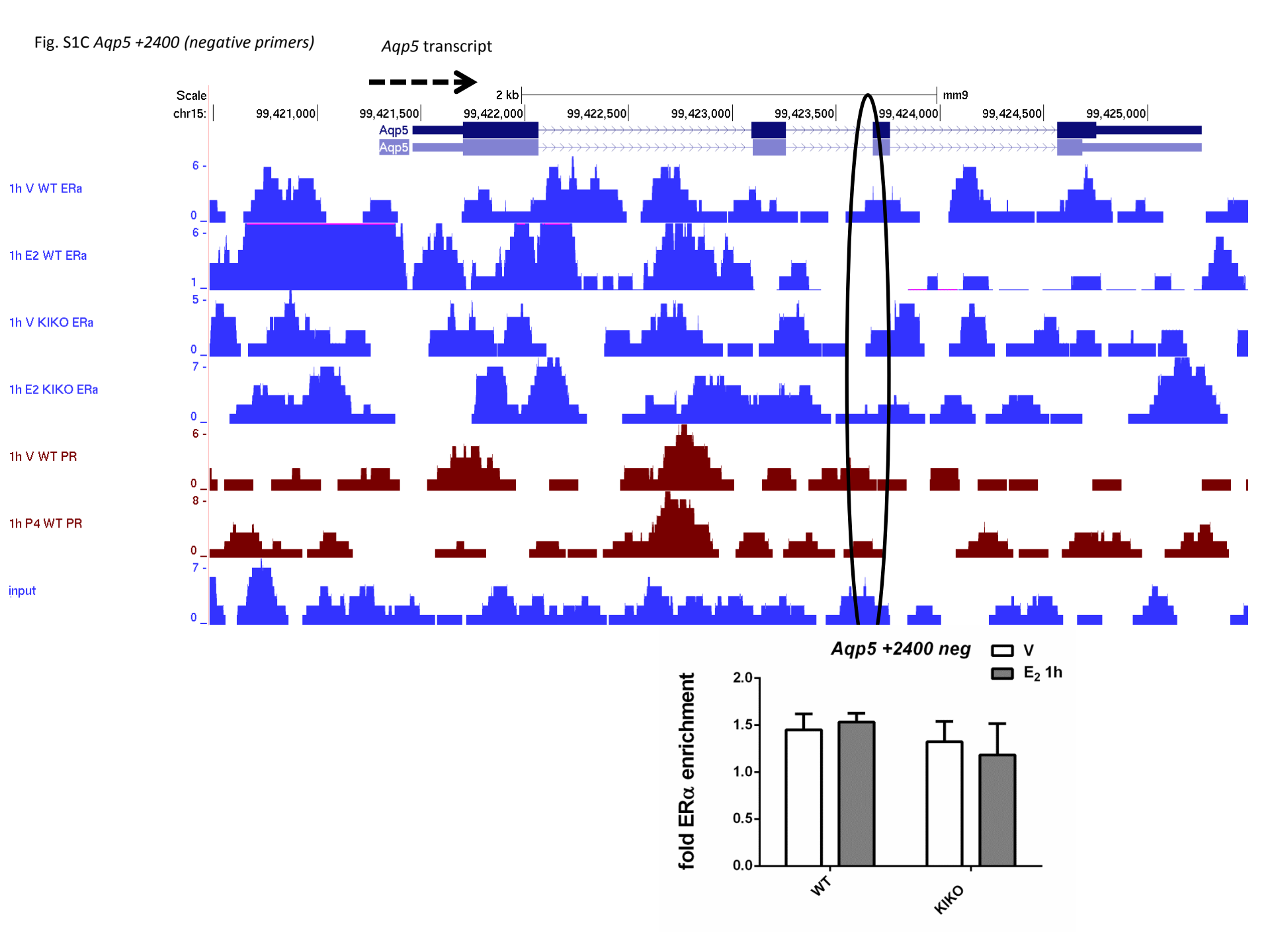

Fig. S2

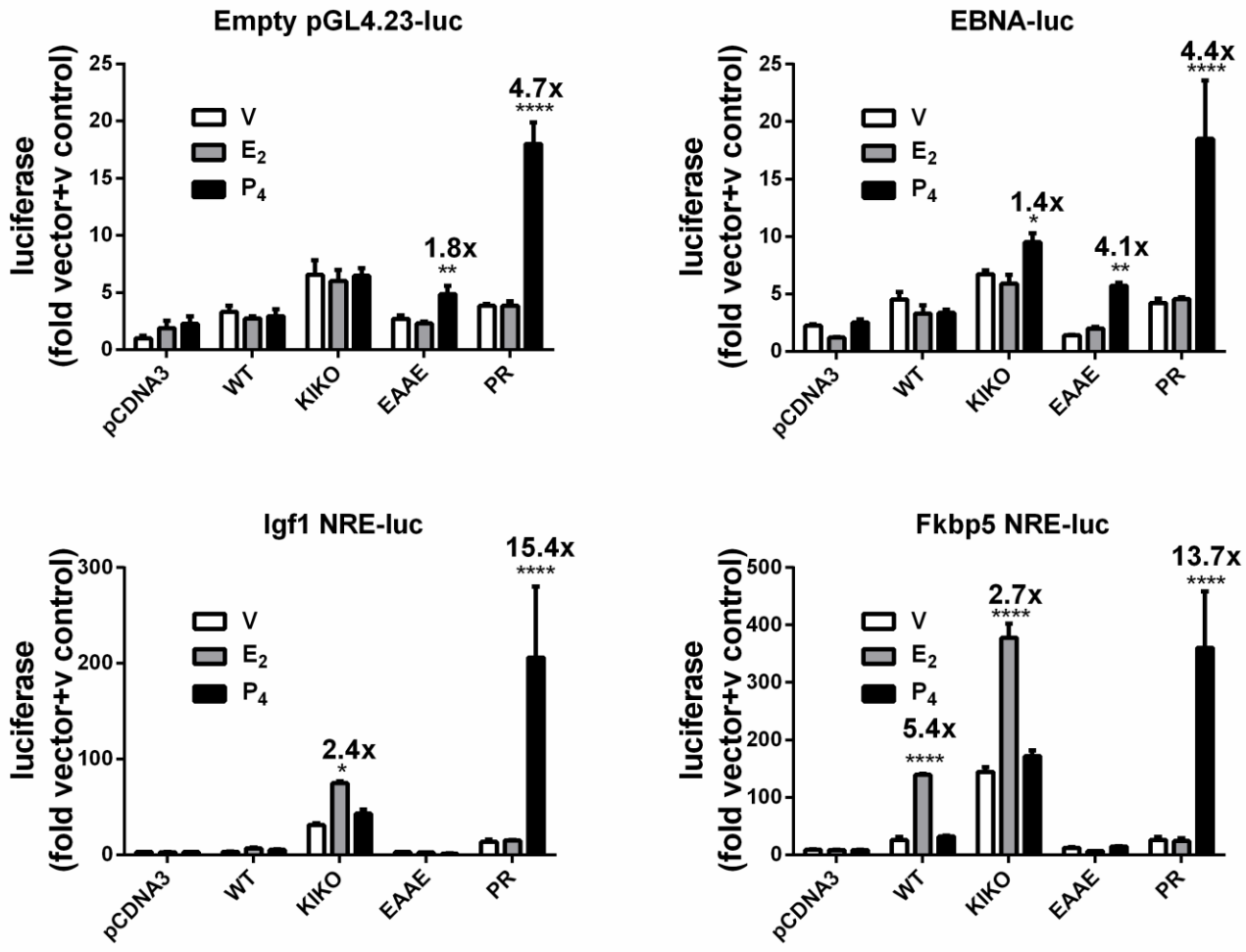
Empty pGL4.23-luc
EBNA-luc
Igf1 NRE-luc
Fkbp5 NRE-luc
luciferase
(fold vector+v control)
V
E2
P4
pCDNA3
WT
KIKO
EAAE
PR
1.8x
4.7x
1.4x
4.1x
4.4x
2.4x
15.4x
5.4x
2.7x
13.7x

Fig. S3

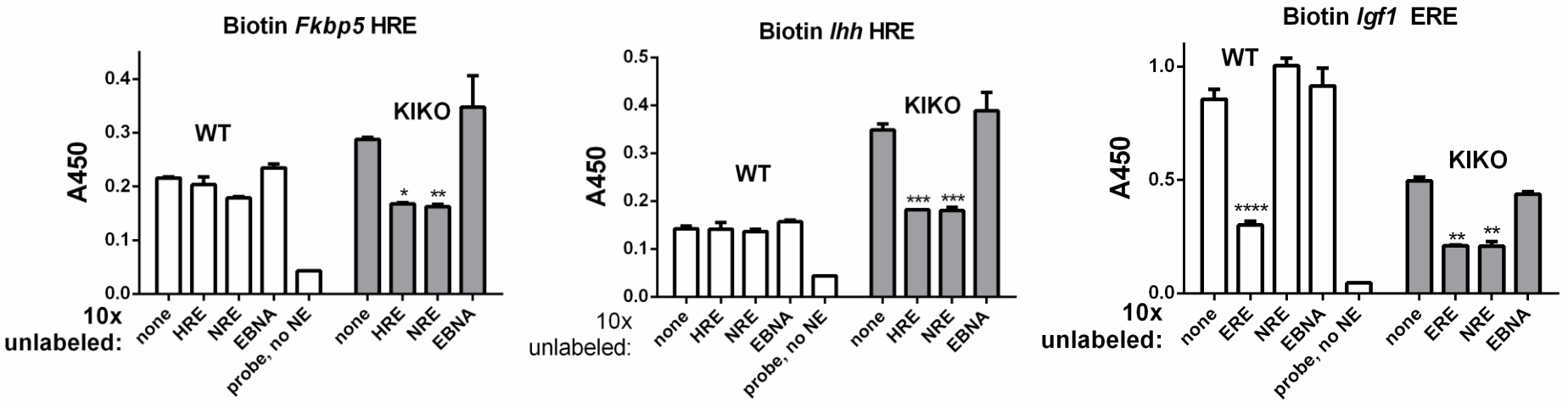
Biotin *Fkbp5* HRE
A450
WT
KIKO
*
**
10x unlabeled:
none
HRE
NRE
EBNA
probe, no NE
Biotin *Ihh* HRE
***
Biotin *Igf1* ERE
****
ERE

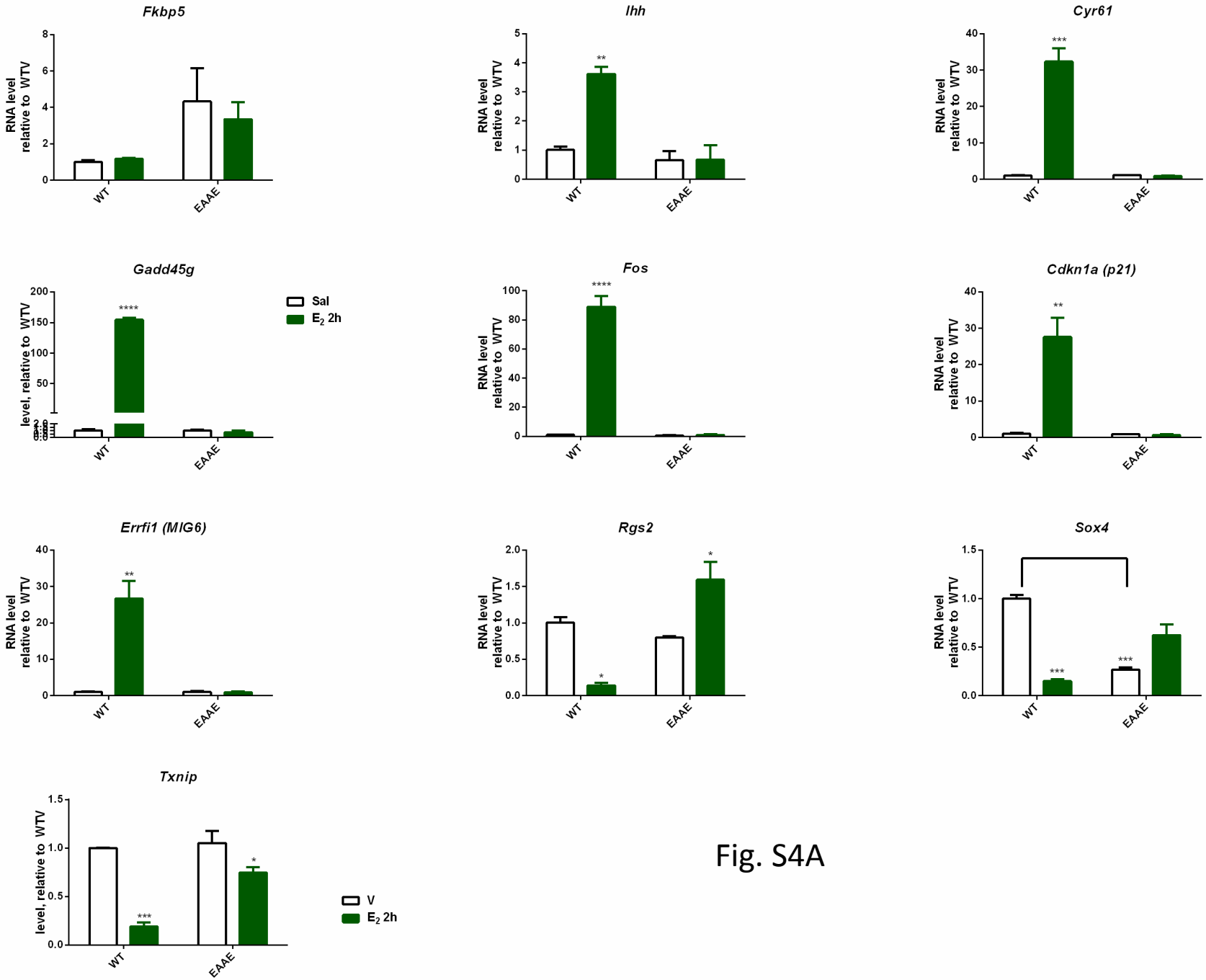
Fkbp5
Ihh
Cyr61
Gadd45g
Fos
Cdkn1a (p21)
Errfi1 (MIG6)
Rgs2
Sox4
Txnip
RNA level relative to WTV
level, relative to WTV
WT
EAAE
Sal
E2 2h
V
E2 2h

Fig. S4A

Fig S4B

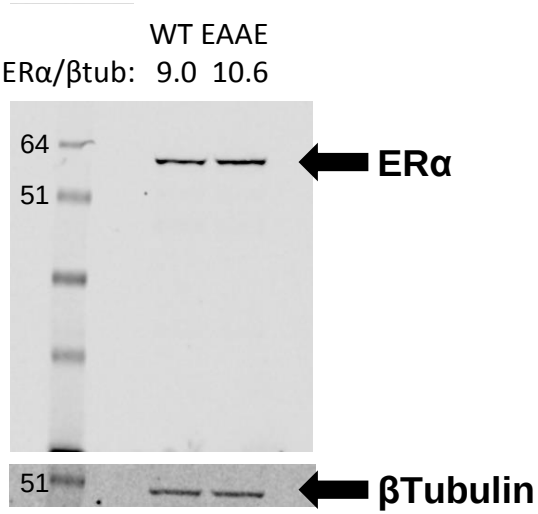

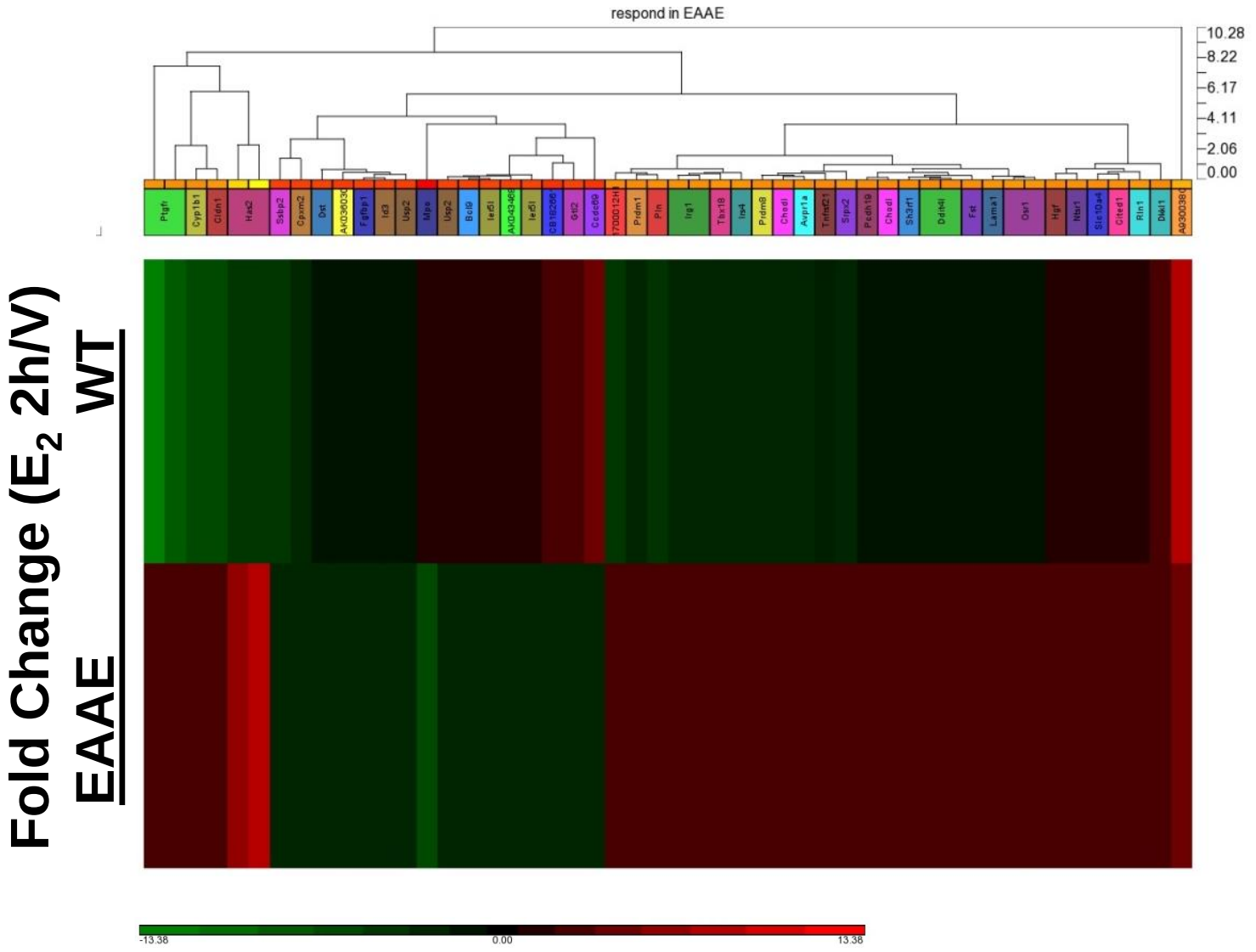
respond in EAAE
10.28
8.22
6.17
4.11
2.06
0.00
Fold Change (E_2 2h/V)
EAAE
WT
-13.38
0.00
13.38

Fig S4C

Fig S4D

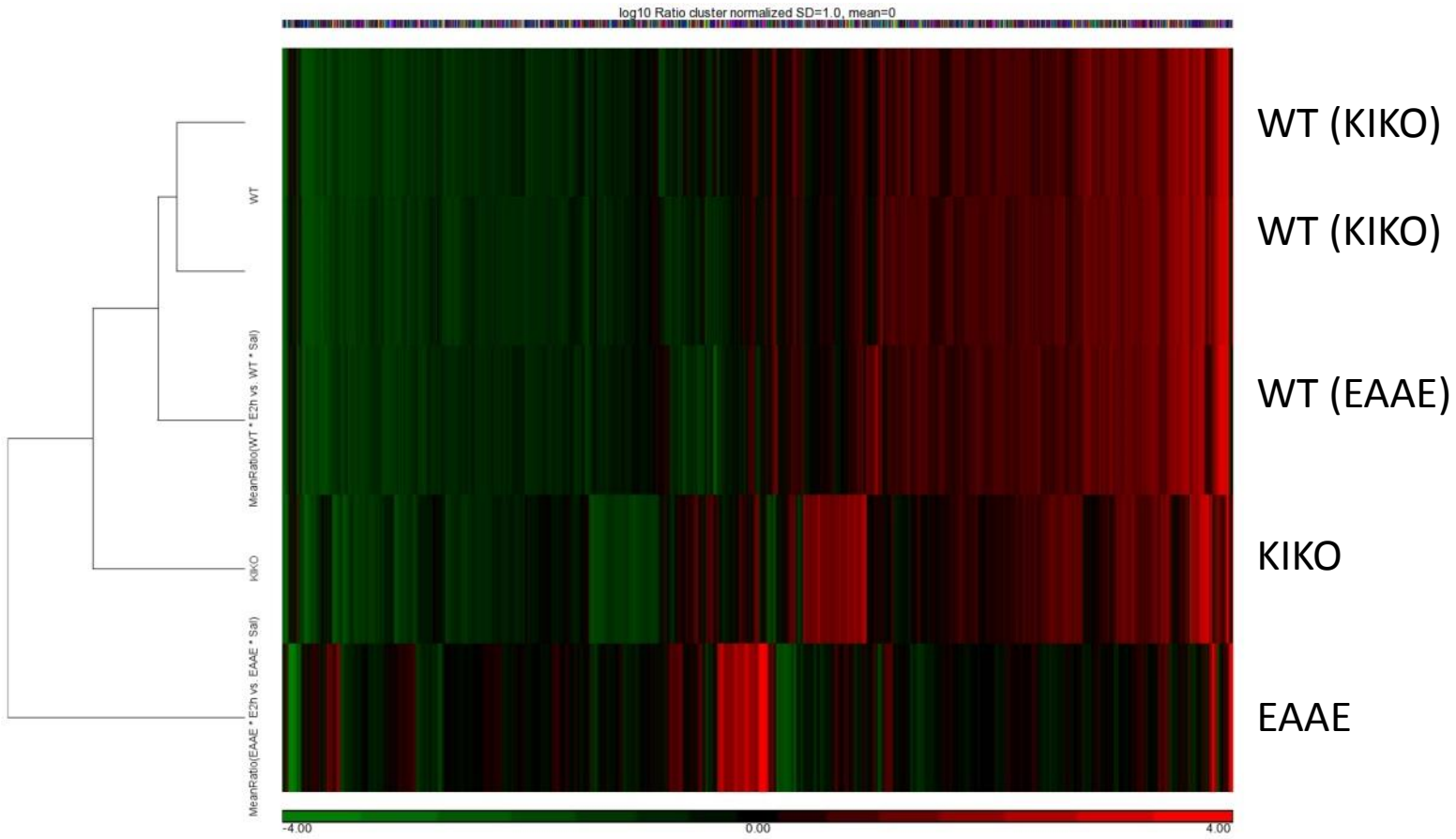
log10 Ratio cluster normalized SD=1.0, mean=0
WT
MeanRatio(WT * E2h vs. WT * Sal)
KIKO
MeanRatio(EAAE * E2h vs. EAAE * Sal)
-4.00
0.00
4.00
WT (KIKO)
WT (KIKO)
WT (EAAE)
KIKO
EAAE

Table S1: Oligonucleotides used insert PREs in luciferase reporter, ChIP –PCR, RT-PCR and mutagenesis

For Luciferase Reporter and DNA Binding Assay:	
Igf1 ERE+	CTGGGCAAGGTCATGATGACCGCTGTATTT
Igf1 ERE-	AAATACAGCGGTCATCATGACCTTGCCCAG
Ihh HRE+	TACGGAAGGAACAGCATGAGCTCCCAGGG
Ihh HRE-	CCCTGGGAGCTCATGCTGTTCCTTCCGTA
Fkbp5 HRE+	GAAGAGCACAGAACACCCTGTTCTGAATGTGG
Fkbp5 HRE-	CCACATTCAGAACAGGGTGTTCTGTGCTCTTC
Igf1 NRE+	CTGGGCAAGATCATGATGATCGCTGTATTT
Igf1 NRE-	AAATACAGCGATCATCATGATCTTGCCCAG
Fkbp5 NRE+	GAAGAGCACAGATCACCCTGATCTGAATGTGG
Fkbp5 NRE-	CCACATTCAGATCAGGGTGATCTGTGCTCTTC
EBNA	ATCTGGGTAGCATATGCTATCCTAA
For ChIP-PCR:	
Igf1 ERE F	TTCCAGCCACCTCTCCACTTAC
Igf1 ERE R	CTGTGGAGCCATTGTTGGATCT
Ihh HRE F	GGGCAGCCACAGAGATCAA
Ihh HRE R	GCATACTTACAGCAGGAGACACTATTTACT
Fkbp5 HRE F	TCTGAATGTGGCTGGCACAT
Fkbp5 HRE R	GCTCCCCACCCCCATTT
Klf15 HRE F	TAACCATCTGGGAAGTGGCT

Klf15 HRE R	GCCACTCTGGAACAGGATG
Aqp5 +2400 neg F	CTCACCGTGACCCCCCTAT
Aqp5 +2400 neg R	CGGGCTGGGTTCATGGA
For RT-PCR	
Klf4 F	GTGCCCCGACTAACCGTTG
Klf4 R	GTCGTTGAACTCCTCGGT
Klf15 F	GGAGTCCAGTCACCACAGG
Klf15 R	ATTTCGGTGACGAGAAGG
EAAE site directed mutagenesis primer 1	GGGTCTGGTCCTGCGAAGGCTGCGCGGCTTTCTTTGCGGAGAGCATTCAAGGACACAATGACTAC
EAAE site directed mutagenesis primer 2	AAGCCGCGCAGCCTTCGCAGGACCAGACCCCCTCATGGTAGCCAGAGGCATAGTCATTGC

Table S2 ChIP-seq data summary

	ER					PR		
	WT Veh	WT E_2	KIKO Veh	KIKO E_2	input	PR Veh	PR P_4	input
sequenced reads	61,593,532	32,117,033	51,125,666	48,508,817	57,614,948	35,628,904	35,585,795	44,458,968
mapped reads	38,357,494	25,913,390	35,163,961	35,360,326	37,569,545	26,103,619	26,739,428	32,323,251
mapped reads, deduplicated	**30,151,013**	**20,399,334**	**28,847,781**	**27,051,778**	**34,039,058**	**17,991,984**	**19,973,075**	**30,611,636**
peaks	5,496	20,792	2,908	18,990	NA	3,541	12,590	NA
estimated fragment length	132	142	120	149	120	138	140	100

Table S3: Motifs significantly enriched ($p<10^{-6}$) in 1h E_2 WT ERα selective vs. 1h E_2 WT ERα+1h E_2 KIKO ERα overlap. GGTCA motifs are highlighted.

Model Name	enrichment p-value
ER_Q6 (ERE)	1.42E-307
ER_Q6_02 (ERE)	1.84E-117
HNF4_Q6_02	1.22E-114
PPARG_Q6	6.41E-113
PPARG_02	6.50E-91
FXR_Q2	7.98E-65
RORA1_01	9.00E-61
ERR1_Q2	3.15E-44
ERR2_01	9.17E-42
PPARA_Q6	1.70E-32
RORA_Q4	2.61E-25
ZNF333_01	2.28E-20
TCF11_01	5.42E-20
SF1_Q6_01	7.80E-18
GCNF_01	6.34E-17
DAX1_01	8.49E-17
NUR77_Q5	3.74E-16
RORA2_01	3.74E-13
AREB6_01	4.77E-13
AREB6_02	5.84E-13
DELTAEF1_01	6.91E-11
OG2_01	5.78E-10
FOXP1_01	9.75E-10
TITF1_Q3	3.20E-09
PXRRXR_02	4.24E-09
DRI1_01	4.43E-09
SIX4_01	2.89E-08
HMGIY_Q3	5.59E-08
SF1_Q6	4.05E-07
NURR1_Q3	6.40E-07

Table S4: Motifs enriched in 1h E2 WT ERα+1h E2 KIKO ERα peaks vs. 1h E2 WT ERα selective peaks ($p<10^{-6}$). Includes potential tethering mediators. Previously described tethering factors are highlighted in blue. HRE motifs are highlighted in yellow.

Model Name	enrichment p-value
AHR_01	7.78E-10
AHRARNT_02	1.86E-08
AHRHIF_Q6	7.66E-10
AP2_Q3	9.44E-37
AP2_Q6	2.79E-36
AP2_Q6_01	2.58E-39
AP2ALPHA_01	1.45E-20
AP2ALPHA_02	1.20E-08
AP2GAMMA_01	4.47E-17
AP4_01	3.74E-10
AP4_Q5	3.04E-11
AP4_Q6	2.16E-17
AR_01	5.24E-39
AR_02	1.11E-30
AR_03	1.07E-37
AR_04	6.98E-46
ARNT_01	2.84E-07
BEN_01	1.41E-13
BEN_02	2.23E-09
CACBINDINGPROTEIN_Q6	1.29E-11
CACD_01	6.33E-12
CEBP_Q2	2.59E-08
CEBP_Q2_01	1.04E-07
CEBPA_01	1.18E-09
CEBPB_02	1.98E-09
CETS1P54_01	1.91E-10
CETS1P54_02	3.39E-14
CETS1P54_03	1.52E-17
CHCH_01	6.56E-27
CKROX_Q2	6.49E-31
CLOCKBMAL_Q6	1.00E-09
CNOT3_01	4.63E-37
CP2_02	4.74E-14
CREB_Q3	8.55E-07
CTCF_01	2.02E-17

CTCF_02	3.22E-11
CTF1_01	3.15E-08
DEAF1_01	1.02E-16
DEAF1_02	9.87E-16
E2F_02	2.64E-14
E2F_Q2	1.47E-31
E2F_Q3_01	2.23E-09
E2F_Q4_01	3.30E-12
E2F_Q6_01	1.03E-13
E2F1_01	7.08E-09
E2F1_Q3	1.50E-10
E2F1_Q3_01	8.70E-20
E2F1_Q4	6.65E-09
E2F1_Q4_01	5.02E-09
E2F1_Q6	3.60E-10
E2F1_Q6_01	3.65E-12
E47_01	1.37E-09
EGR_Q6	1.34E-16
EGR1_01	1.28E-15
EGR2_01	2.58E-12
EGR3_01	1.41E-13
ELK1_01	7.14E-08
ELK1_02	1.87E-23
ELK1_04	1.65E-10
ETF_Q6	1.36E-32
ETS1_B	7.41E-08
ETS2_Q6	4.78E-11
FPM315_01	1.09E-34
GABP_B	1.55E-17
GABPALPHA_Q4	2.26E-22
GADP_01	2.01E-15
GKLF_02	1.58E-15
GR_01	3.79E-29
GR_Q6	1.44E-17
HEB_Q6	1.85E-14
HEN1_01	2.51E-14
HEN1_02	3.95E-18
HIC1_02	2.16E-20
HIC1_03	8.65E-11
HIF1_Q3	1.36E-11
HIF1_Q5	2.08E-07

IK_Q5	3.58E-16
KID3_01	1.72E-07
KROX_Q6	1.85E-38
LBP1_Q6	2.62E-24
LBP9_01	1.52E-10
MAZ_Q6	4.23E-16
MAZR_01	5.82E-13
MEF2_02	9.40E-07
MOVOB_01	6.30E-19
MTF1_Q4	8.09E-13
MYCMAX_03	4.31E-07
MYCMAX_B	9.37E-12
MYOD_Q6_01	5.00E-07
MYOGNF1_01	9.82E-09
MZF1_01	6.99E-07
NERF_Q2	6.48E-11
NEUROD_01	6.89E-10
NEUROD_02	3.62E-15
NF1_Q6	4.18E-30
NF1_Q6_01	1.51E-19
NGFIC_01	1.47E-17
NRSF_01	1.31E-07
NRSF_Q4	6.31E-12
P300_01	9.86E-13
P53_04	1.33E-09
PAX4_01	3.14E-12
PAX5_01	2.58E-08
PR_01	3.39E-25
PR_02	3.01E-28
RBPJK_Q4	9.30E-07
REST_01	6.08E-17
RNF96_01	1.25E-24
SAP1A_01	3.48E-18
SP1_01	3.28E-09
SP1_02	7.01E-21
SP1_Q2_01	1.53E-26
SP1_Q4_01	7.74E-25
SP1_Q6	2.78E-25
SP1_Q6_01	1.07E-23
SP1SP3_Q4	2.25E-30
SP3_Q3	3.39E-09

SP4_Q5	2.58E-24
SPZ1_01	1.79E-12
SREBP2_Q6	2.10E-08
STAT1_01	3.83E-12
STAT1_03	1.54E-08
STAT1_05	1.95E-09
STAT3_01	7.71E-09
STAT3_02	1.74E-10
STAT3_03	8.04E-18
TAL1_Q6	1.33E-12
TAL1ALPHAE47_01	1.15E-08
TFIII_Q6	2.13E-09
USF_01	9.49E-07
USF_Q6	7.91E-11
WT1_Q6	8.42E-26
ZBED6_01	3.22E-19
ZBRK1_01	8.51E-10
ZF5_01	3.53E-18
ZF5_B	1.17E-11
ZFP281_01	1.45E-16
ZFX_01	1.30E-49
ZNF219_01	1.22E-20

Table S5

WTWT and KIWT differ significantly in uterine weight from 7 weeks through 18 weeks.

Age-adjusted mean uterine weights, excluding animals ≤ 4 weeks

	Age-adjusted mean uterine weight (mg)± s.e.		KIWT vs. WTWT
Age (weeks)	KIWT	WTWT	p-value
3			
4			
5	51.1 ± 9.0	67.7 ± 10.7	0.2388
6	73.5 ± 6.9	69.3 ± 8.6	0.7061
7	94.0 ± 5.6	70.6 ± 7.9	0.0170
8	112.7 ± 5.1	71.5 ± 8.2	<0.0001
9	129.6 ± 5.4	72.2 ± 8.8	<0.0001
10	144.7 ± 5.8	72.5 ± 9.2	<0.0001
11	157.9 ± 6.3	72.5 ± 9.3	<0.0001
12	169.3 ± 6.6	72.2 ± 9.0	<0.0001
13	178.8 ± 6.7	71.6 ± 8.6	<0.0001
14	186.5 ± 6.6	70.7 ± 8.4	<0.0001
15	192.4 ± 6.4	69.4 ± 9.0	<0.0001
16	196.4 ± 6.4	67.9 ± 11.0	<0.0001
17	198.6 ± 6.7	66.0 ± 14.4	<0.0001
18	199.0 ± 7.6	63.8 ± 19.0	<0.0001

Uterine weights were measured in peri-pubertal KIWT females, revealing significant enlargement occurs beginning at 7 weeks of age, following the onset of exposure to cycling ovarian hormones at 4 weeks of age. Therefore, the abnormal uterine enlargement likely reflects the biological consequence of inappropriate estrogen-dependent transcriptional regulation mediated by the DBD mutation.

Table S6. Summary of DNA binding (DNA) and reporter gene (Luc) activity of motifs tested. KIKO RE shows nucleotides that exhibit activity with KIKO ER

		DNA		Luc	
	12345 54321	WT	KIKO	WT	KIKO
(ER) ERE:	GGTCAnnnTGACC				
(PR,GR,AR)HRE:	GAACAnnnTGTTC				
KIKO RE:	GnnCAnnnTGnnC				
Fkbp5 HRE:	GAACACCCTGTTC	-	+	+	++
Fkbp5 NRE:	GATCACCCTGATC	-	+	+	++
Igf1 ERE:	GGTCATGATGACC	+	+	++	-
Igf1 NRE:	GATCATGATGATC	-	+	-	+
Ihh HRE:	GAACAGCATGAGC	-	+	-	+
EBNA:	ATCTGGGTAGCATATGCTATCCTAA	-	-	-	-